

CHEMISTRY

AN **ASIAN** JOURNAL

www.chemasianj.org

Accepted Article

Title: Acid-Base Switchable [2]- and [3]Rotaxane Molecular Shuttles with Benzimidazolium and Bis(pyridinium) Recognition Sites

Authors: Kelong Zhu; Nicholas Vukotic; Stephen J. Loeb

This manuscript has been accepted after peer review and the authors have elected to post their Accepted Article online prior to editing, proofing, and formal publication of the final Version of Record (VoR). This work is currently citable by using the Digital Object Identifier (DOI) given below. The VoR will be published online in Early View as soon as possible and may be different to this Accepted Article as a result of editing. Readers should obtain the VoR from the journal website shown below when it is published to ensure accuracy of information. The authors are responsible for the content of this Accepted Article.

To be cited as: Chem. Asian J. 10.1002/asia.201601179

Link to VoR: <http://dx.doi.org/10.1002/asia.201601179>

A Journal of



A sister journal of *Angewandte Chemie*
and *Chemistry – A European Journal*

WILEY-VCH

Acid-Base Switchable [2]- and [3]Rotaxane Molecular Shuttles with Benzimidazolium and Bis(pyridinium) Recognition Sites

Kelong Zhu^{*[a]}, V. Nicholas Vukotic^[b] and Stephen J. Loeb^{*[b]}

Abstract: For the purpose of developing higher level mechanically interlocked molecules (MIMs), such as molecular switches and machines, a new rotaxane system was designed in which both the 1,2-bis(pyridinium)ethane and benzimidazolium recognition templating motifs were combined. These two very different recognition sites were successfully incorporated into [2]rotaxane and [3]rotaxane molecular shuttles which were fully characterized by ¹H NMR, 2D EXSY, single crystal X-ray diffraction and VT NMR analysis. By utilizing benzimidazolium as both a recognition site and stoppering group it was possible to create, not only, an acid/base switchable [2]rotaxane molecular shuttle (energy barrier 20.9 kcal·mol⁻¹) but also a [3]rotaxane molecular shuttle that displays unique dynamic behavior involving the simultaneous motion of two macrocyclic wheels on a single dumbbell. This study provides new insights into the design of switchable molecular shuttles. Due to the unique properties of benzimidazoles, such as fluorescence and metal coordination, this new type of molecular shuttle may find further applications in developing functional molecular machines and materials.

Introduction

Molecular shuttles and switches derived from mechanically interlocked molecules (MIMs) are attractive outcomes from supramolecular chemistry.^[1] They have proven to have potential applications in, not only, biomimetic synthesis,^[2] catalysis,^[3] sensors,^[4] and drug delivery,^[5] but also advanced materials including liquid crystals,^[6] smart polymers,^[7] computer memory,^[8] and metal-organic frameworks (MOFs).^[9] For the efficient fabrication of MIMs, templated synthesis,^[10] which involves intermolecular recognition, is usually employed. Moreover, by the judicious combination of different recognition motifs, one can develop artificial molecular switches which operate under external stimuli at the molecular level.

In the last two decades, electron deficient pyridinium salts have been broadly used as recognition templates for developing MIMs with crown ethers or cryptands due to their straightforward synthesis and strong binding ability.^[11] In particular, we reported that 1,2-bis(pyridinium)ethane dication (1^{2+}) could be used as axles to form [2]pseudorotaxanes with 24-membered crown ethers such as commercially available dibenzo[24]-crown-8 (**DB24C8**).^[11c] This has also been shown to be a versatile motif for the formation of [2]rotaxanes,^[12] [3]rotaxanes,^[13] [3]catenanes,^[14] molecular shuttles,^[15] branched [n]rotaxanes ($n = 2-4$)^[16] and metal-organic rotaxane frameworks (MORFs).^{[9], [17]} Imidazolium and benzimidazolium cations have also been found to complex macrocycle hosts such as crown ethers, cryptands and pillararenes.^[18] In this regard, we developed a series of T-shaped benzimidazolium cations (e.g. [2-H]⁺) which act as an efficient template for the formation of [2]pseudorotaxanes with crown ethers. Based on this new recognition motif, we further developed an H-shaped molecular shuttle^[19] which could be incorporated into a MOF showing for the first time that a molecular shuttle could operate in the solid-state.^[9]

For the purpose of developing higher level MIMs, such as molecular switches and machines, a new rotaxane system was designed in which both the 1,2-bis(pyridinium)ethane and benzimidazolium recognition templating motifs are combined; see Figure 1.^[19b, 19c] Due to the different binding strengths of the two types of recognition sites, it was anticipated that it would be possible to translocate macrocyclic wheels between the different sites in a controlled manner. Herein, we report [2]- and [3]rotaxanes constructed from a combination of both recognition motifs and **DB24C8**. The shuttling dynamics of these molecular shuttles were also examined with acid/base as the external stimulus.

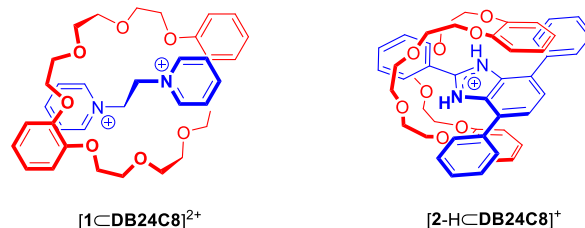


Figure 1. Simple examples of [2]pseudorotaxanes based on 1,2-bis(pyridinium)ethane and benzimidazolium axles and **DB24C8** wheels. Anions are omitted for clarity.

[a] Prof. Dr. K. Zhu
School of Chemistry and Chemical Engineering
Sun Yat-Sen University
Guangzhou, P. R. China, 510275
E-mail: zhukelong@mail.sysu.edu.cn

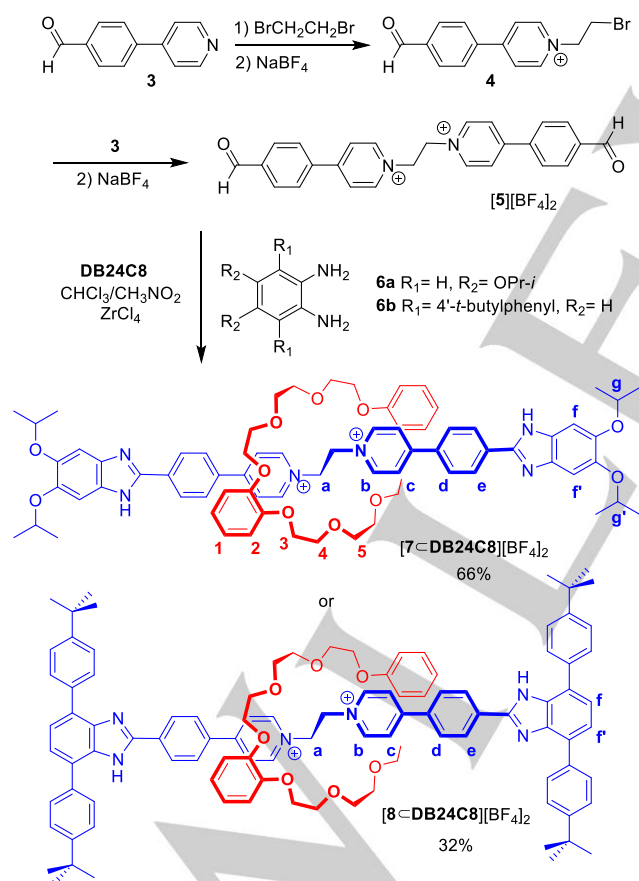
[b] Dr. V. N. Vukotic, Prof. Dr. S. J. Loeb
Department of Chemistry and Biochemistry
University of Windsor
Windsor, Ontario, Canada, N9B 3P4
E-mail: loeb@uwindsor.ca

Supporting information for this article is given via a link at the end of the document.

Results and Discussion

[2]Rotaxanes

The [2]rotaxanes $[7\text{-DB24C8}]^{2+}$ and $[8\text{-DB24C8}]^{2+}$ were prepared as outlined in Scheme 1. 4-(4'-Formylphenyl)pyridine, **3**^[20] was alkylated in 1,2-dibromoethane to give 1-bromoethyl-4-(4'-formylphenyl)pyridinium **4**⁺ which was followed by another alkylation to give the dialdehyde bispyridinium thread **5**²⁺. The threading-followed-by-stoppering method was employed to synthesize the [2]rotaxanes. Firstly, one equivalent of **5**²⁺ was mixed with four equivalents of **DB24C8** in solution to maximize [2]pseudorotaxane formation and then the [2]pseudorotaxane was condensed with 2.2 equivalents of 4,5-di-isopropoxy-1,2-diamine, **6a** in the presence of a catalytic amount of ZrCl_4 to produce the [2]rotaxane $[7\text{-DB24C8}]^{2+}$ in 66% yield. Similarly, [2]rotaxane $[8\text{-DB24C8}]^{2+}$ was obtained in a yield of 32% by using 1,2-diamino-3,6-di(4-*t*-butylphenyl)benzene, **6b**^[19c] as the stopper. In both cases, the naked dumbbell **7**²⁺ or **8**²⁺ was isolated as the main by-product. The formation of [2]rotaxane was confirmed by NMR spectroscopy and mass spectrometric analysis for each.



Scheme 1. Synthesis of [2]rotaxanes $[7\text{-DB24C8}]^{2+}$ and $[8\text{-DB24C8}]^{2+}$.

[2]Rotaxane Molecular Shuttles

A comparison of the ^1H NMR spectra of [2]rotaxane $[7\text{-DB24C8}]^{2+}$ and the dumbbell **7**²⁺ is shown in Figure 2. The higher frequency chemical shifts of protons a ($\Delta\delta = +0.40$ ppm) and b ($\Delta\delta = +0.45$ ppm) for **7**²⁺ likely result from hydrogen bonding of these protons to oxygen atoms of the crown ether. Significant upfield chemical shifts were observed for protons c ($\Delta\delta = -0.35$ ppm) and d ($\Delta\delta = -0.32$ ppm) which indicates π -stacking of the electron-rich benzo groups of the crown ether with the electron-poor pyridinium rings of the dumbbell. All of this spectral evidence indicates that **7**²⁺ and **DB24C8** form structures similar to other 1,2-bis(pyridinium)ethane/crown ether rotaxanes, i.e. the crown ether adopts an S-shaped conformation and is seated in the middle of the 1,2-bis(pyridinium)ethane axle to maximize noncovalent interactions.^[12] [2]Rotaxane formation was also confirmed by mass spectrometric analysis; the observed m/z of 625.3164 corresponds to $[7\text{-DB24C8}]^{2+}$.

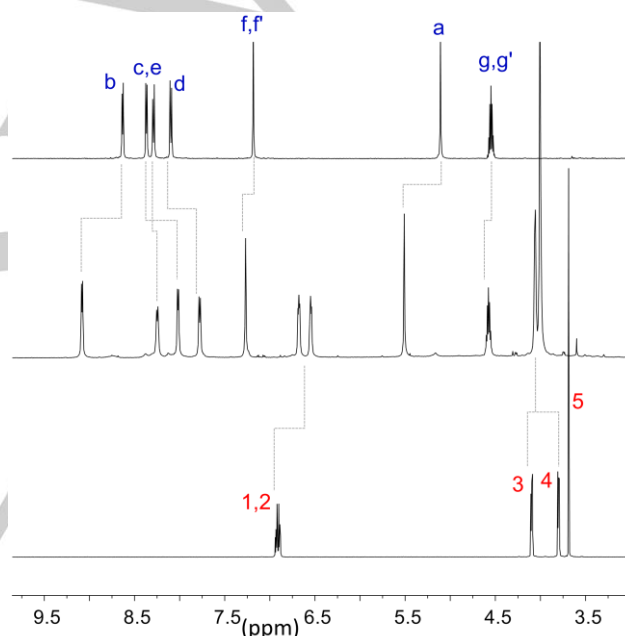


Figure 2. Partial ^1H NMR spectra (500 MHz, CD_3CN , 298K) for **7**²⁺ (top), $[7\text{-DB24C8}]^{2+}$ (middle), and **DB24C8** (bottom). See Scheme 1 for labelling.

Single crystals of $[7\text{-DB24C8}][\text{CF}_3\text{SO}_3]_2$ suitable for X-ray diffraction were obtained by slow evaporation of a methanol solution of the compound; BF_4^- anions were replaced by CF_3SO_3^- anions in order to grow suitable crystals of the cation. The solid-state structure of the [2]rotaxane is shown in Fig 3 (top). The crown ether adopts an S-shaped conformation and is located around the 1,2-bis(pyridinium)ethane site. It is also clear from the structure that the aromatic rings of the crown ether are involved in significant π -stacking interactions with the aromatic groups of the pyridinium axle. The four ethylene protons of the $-\text{NCH}_2\text{CH}_2\text{N}-$ linkage form H-bonds with O-atoms of the crown ether which is consistent with what was observed in the ^1H NMR spectrum. Thus,

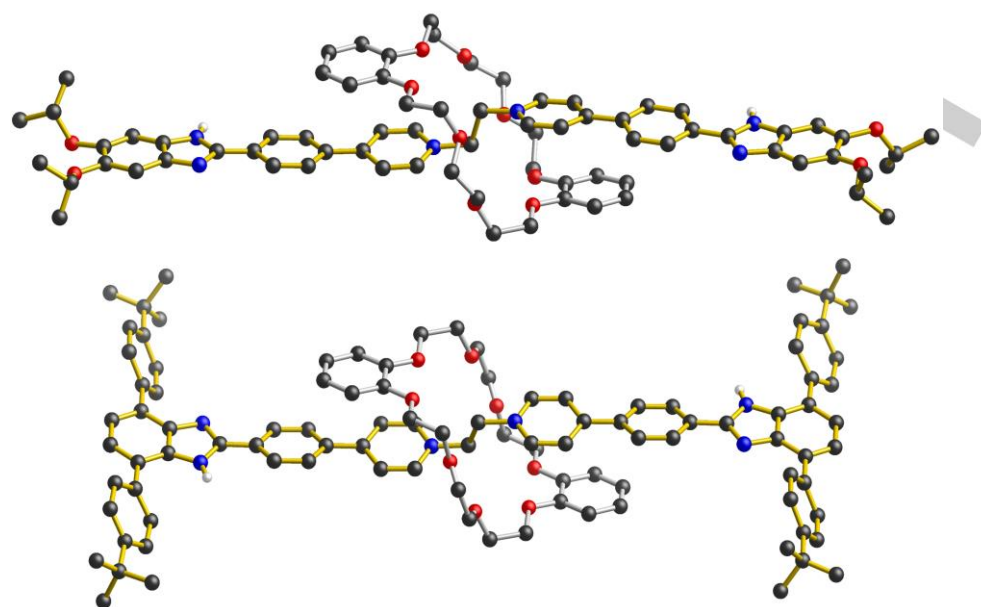


Figure 3. Single crystal X-ray structures of: Top, rotaxane $[7\text{-DB24C8}][\text{CF}_3\text{SO}_3]_2(\text{CH}_3\text{OH})_2$ and bottom, rotaxane $[8\text{-DB24C8}][\text{CF}_3\text{SO}_3]_2(\text{CH}_3\text{CN})_6$. Color key: red = oxygen, blue = nitrogen, black = carbon, white = hydrogen. Only NH H-atoms are shown and all anions and solvent molecules are omitted for clarity.

this structure can be considered as the static state with the lowest energy conformation; *i.e.* no shuttling occurs.

Since the readily incorporated benzimidazole stopper can be protonated to give a benzimidazolium cation which can then act as a secondary binding site, the acid/base switching ability $[7\text{-DB24C8}]^{2+}$ was tested. After the addition of two equivalents of tetrafluoroboric acid to an acetonitrile solution of $[7\text{-DB24C8}]^{2+}$, only small changes were observed in the ^1H NMR spectrum (Figure S1). The biggest difference was the appearance of a characteristic singlet at 13.1 ppm corresponding to the *NH* proton of the benzimidazolium group. However, only very small

downfield chemical shifts of the aromatic protons a and b were observed for $[7\text{-H}_2\text{-DB24C8}]^{4+}$. This was rationalized as being due to a slight enhancement of the H-bonding of the now protonated dumbbell $[7\text{-H}_2]^{4+}$ to the crown ether. No significant chemical shift changes were observed for the crown ether protons. These limited spectral changes indicate that the crown ether remains exclusively at the 1,2-bis(pyridinium)ethane recognition site even after protonation. To verify this interpretation, a simple model, di-isopropoxy benzimidazolium $9a^+$ (see SI) was synthesized and an association constant of 43 M^{-1} measured for [2]pseudorotaxane formation with **DB24C8**. This is much weaker

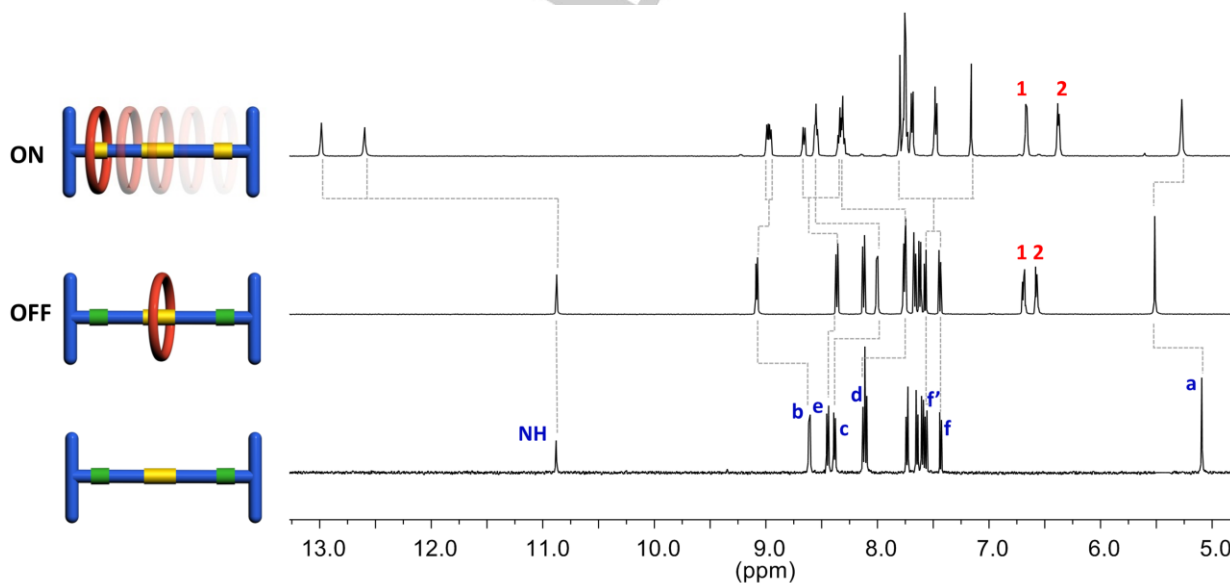


Figure 4. Partial ^1H NMR spectra (500 MHz, CD_3CN , 298K) of 8^{2+} (bottom), $[8\text{-DB24C8}]^{2+}$ (middle), and $[8\text{-H}_2\text{-DB24C8}]^{4+}$ (top). See Scheme 1 for labelling.

than the value of 230 M^{-1} previously reported for the parent 1,2-bis(4-phenylpyridinium)ethane dication (see Table S1).^[21] Thus, we can infer that for the protonated dumbbell $[7\text{-H}_2]^{4+}$, the **DB24C8** wheel favors the 1,2-bis(pyridinium)ethane recognition site.

The H-shaped [2]rotaxane $[8\text{-DB24C8}]^{2+}$ was synthesized by using the same approach as for $[7\text{-DB24C8}]^{2+}$ but including larger and more rigid *t*-butylphenyl groups. Comparison of the ^1H NMR spectrum of [2]rotaxane $[8\text{-DB24C8}]^{2+}$ with the dumbbell 8^{2+} is shown in Figure 4. The higher frequency chemical shifts of protons a ($\Delta\delta = +0.42\text{ ppm}$) and b ($\Delta\delta = +0.47\text{ ppm}$) for 8^{2+} are the result of H-bonding of these protons to oxygen atoms on the crown ether. Significant upfield chemical shifts were observed for protons c ($\Delta\delta = -0.38\text{ ppm}$) and d ($\Delta\delta = -0.36\text{ ppm}$) indicative of π -stacking of the benzo group of the crown ether with the pyridinium rings. Again, no change in the signal for the benzimidazole NH proton was observed. This spectral evidence indicates that $[8\text{-DB24C8}]^{2+}$ has a structure similar to $[7\text{-DB24C8}]^{2+}$ and this was verified by an X-ray crystal structure.

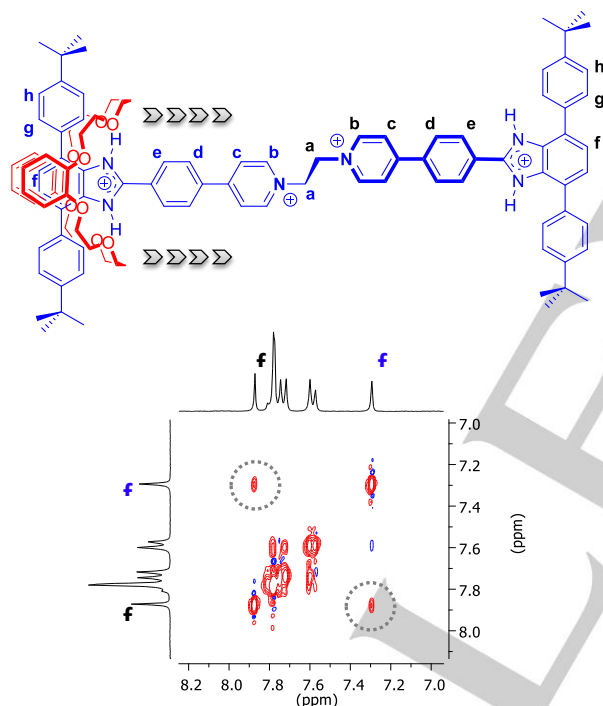


Figure 5. A diagram illustrating the shuttling of the wheel in [2]rotaxane $[8\text{-H}_2\text{-DB24C8}]^{4+}$ (top) and a 2D ^1H - ^1H EXSY spectrum of $[8\text{-H}_2\text{-DB24C8}]^{4+}$ (CD_3CN , 300 MHz, 338K, $\tau_m = 0.5\text{ s}$).

As shown in Figure 3 (bottom), the crown ether wheel adopts an S-shaped conformation and is seated on the 1,2-bis(pyridinium)ethane site. The aromatic rings of the crown ether are involved in significant π -stacking interactions with the aromatic groups of the pyridinium axle as designed. The four central ethylene protons form H-bonds with O-atoms of the crown ether which is consistent with observations from the ^1H NMR experiments. Again, similar to $[7\text{-DB24C8}]^{2+}$, this structure can

be described as the state with the lowest energy conformation where no shuttling occurs.

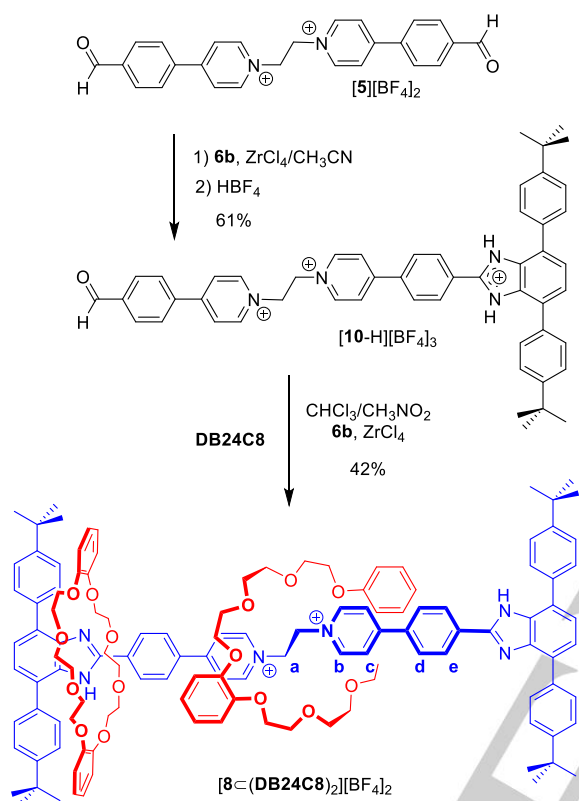
However, in stark contrast to $[7\text{-DB24C8}]^{2+}$, very different spectral changes were observed upon protonation of $[8\text{-DB24C8}]^{2+}$ to give $[8\text{-H}_2\text{-DB24C8}]^{4+}$. As shown in Figure 4 (top), with two equivalents of acid, two sets of proton signals are observed for $[8\text{-H}_2\text{-DB24C8}]^{4+}$ which indicates an unsymmetrical environment for the dumbbell. Two signals for the NH protons were observed corresponding to both complexed and free benzimidazolium sites. At the same time, proton a is upfield shifted to 5.25 ppm which is close to the signal for free 8^{2+} indicating the absence of the wheel at the 1,2-bis(pyridinium)ethane site. Significant upfield chemical shifts were also observed for proton f and benzo proton i indicating π -stacking of the benzo moieties on the benzimidazolium units. These significant spectral changes infer that the ring has moved from the central 1,2-bis(pyridinium)ethane site to the newly formed benzimidazolium site. This is consistent with the fact that the association constant for [2]pseudorotaxane formation of the simple model 2,4,7-triphenylbenzamidazolium cation with **DB24C8**, previously measured to be 1780 M^{-1} ,^[19a] is much greater than the value of 230 M^{-1} reported for the parent 1,2-bis(4-phenylpyridinium)ethane dication.^[21] Furthermore, the presence of two benzimidazolium recognition sites at the termini of the dumbbell means that this protonated rotaxane could potentially be operating as degenerate molecular shuttle. Indeed, exchange signals for the complexed and free proton f were observed in a 2D EXSY experiment which confirms that the macrocyclic wheel is indeed shuttling between the two benzimidazolium sites at a rate slower than the NMR timescale.^[22] At 298 K, a shuttling rate of $4.8 \times 10^{-5}\text{ s}^{-1}$ ($7.8 \times 10^{-2}\text{ s}^{-1}$ at 338 K), was measured which corresponds to an energy barrier of $20.9\text{ kcal}\cdot\text{mol}^{-1}$ (see SI). Further studies showed that the protonated rotaxane can readily be neutralized back to the original dication which has a static co-conformation where no shuttling occurs (Figure S10). Thus, we can conclude that the combination of T-shaped benzimidazolium and 1,2-bis(pyridinium)ethane recognition sites allows for formation of an acid/base switchable [2]rotaxane molecular shuttle; i.e two distinct cations with different charges, linked by changes in pH represent ON (shuttling) and OFF (no shuttling) states.

[3]Rotaxane Molecular Shuttle

Encouraged by the successful formation of [2]rotaxanes from the combination of T-shaped benzimidazolium and 1,2-bis(pyridinium)ethane recognition sites, we attempted to expand this novel chemistry into a more sophisticated system – a [3]rotaxane which consists of one dumbbell 8^{2+} with three recognition sites and two **DB24C8** wheels.

Accordingly, the threading-followed-by-stoppering method was employed to synthesize the [3]rotaxane $[8\text{-DB24C8}]_2^{2+}$. As outlined in Scheme 2, firstly, the monoaldehyde axle 10-H^{3+} was obtained by condensation of an excess of dialdehyde axle 5^{2+} with the diamino compound **6b** followed by protonation with one equivalent of tetrafluoroboric acid. After one equivalent of $[10\text{-H}]^{3+}$ was mixed with four equivalents of **DB24C8** in solution, the resulting [3]pseudorotaxane was condensed with one equivalent

of **6b** in the presence of a catalytic amount of ZrCl_4 , followed by neutralization with proton sponge to produce the [3]rotaxane $[\mathbf{8c}(\text{DB24C8})_2]^{2+}$ in a yield of 42%. The [2]rotaxane $[\mathbf{8c}(\text{DB24C8})]^{2+}$ and the dumbbell $\mathbf{8}^{2+}$ were found to be the main by-products. The formation of [3]rotaxane $[\mathbf{8c}(\text{DB24C8})_2]^{2+}$ was confirmed by NMR spectroscopic and mass spectrometry analysis. (see Figure S5)



Scheme 2. Synthesis of [3]rotaxane molecular shuttle $[\mathbf{8c}(\text{DB24C8})_2]^{2+}$.

The ^1H NMR spectrum of [3]rotaxane $[\mathbf{8c}(\text{DB24C8})_2]^{2+}$ at 298 K is shown in Figure 6 (middle). Only one set of signals for both rings and dumbbell were observed which indicates either a static state or a dynamic process faster than the NMR timescale. The NH proton was found to have a chemical shift 0.27 ppm downfield compared to the dumbbell which could be due to hydrogen bonding of the NH to oxygen atoms on the macrocyclic wheel; Figure 6 (top).^[23] In addition, the ethylene proton signal a also shifted downfield by 0.38 ppm which is characteristic for threading of a **DB24C8** wheel onto the 1,2-bis(pyridinium)ethane site. Considering only one set of proton signal was observed, the [3]rotaxane is most likely a degenerate molecular shuttle where the two wheels are translating simultaneously. This molecular shuttling behavior was further characterized by a VT NMR study. Upon cooling a solution of $[\mathbf{8c}(\text{DB24C8})_2]^{2+}$ in CD_3CN , the proton signal for the NH starts to broaden and eventually splits into two signals at 233 K (Figure S8). In order to improve the solubility of $[\mathbf{8c}(\text{DB24C8})_2]^{2+}$ at low temperature, a solution of $[\mathbf{8c}(\text{DB24C8})_2]^{2+}$ in CD_2Cl_2 was used for the VT NMR study. As shown in Figure 7, a coalescence temperature was accessible at 230 K. Two separate NH signals, at 12.13 and 10.48 ppm, were obtained after cooling the sample to 204 K indicating a reduction in symmetry for the chemical environments of the dumbbell due to an uneven distribution of the crown ether wheels. This was further supported by the observation of separate signals for the benzo protons 1 and 2. The signal at 6.5 ppm is similar to the chemical shift (6.6 ppm) observed for [2]rotaxane $[\mathbf{8c}(\text{DB24C8})]^{2+}$ in which the wheel resides exclusively on the central 1,2-bis(pyridinium)ethane recognition site. By using the coalescence temperature method, an energy barrier of 9.9 $\text{kcal}\cdot\text{mol}^{-1}$ and a rate of $3.4 \times 10^5 \text{ s}^{-1}$ were estimated for the simultaneous shuttling of both the wheels at 298 K.

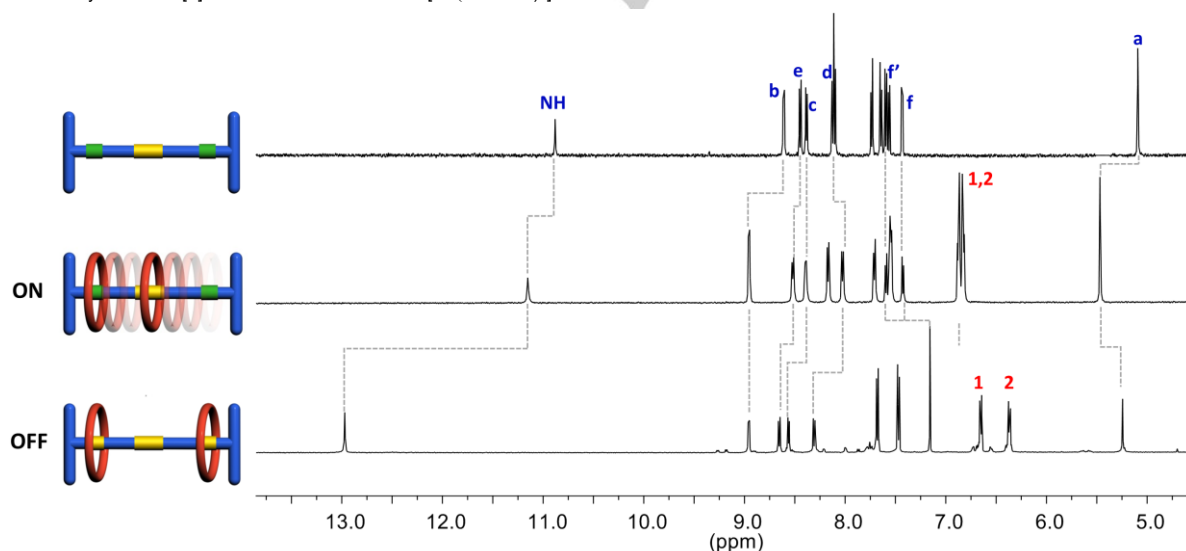


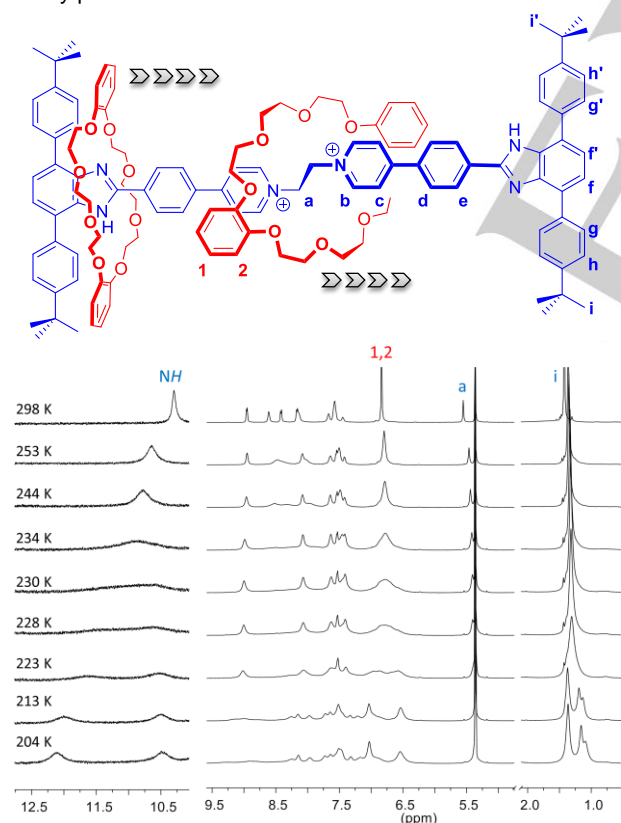
Figure 6 Partial proton NMR spectra (500 MHz, CD_3CN , 298K) of (a) $\mathbf{8}^{2+}$, (b) $[\mathbf{8c}(\text{DB24C8})]^{2+}$, and (c) $[\mathbf{8-H}_2\text{c}(\text{DB24C8})]^{2+}$. See Scheme 1 for labelling.

Table 1. Proton chemical shift changes for the dumbbell protons of 8^{2+} upon formation of [2]rotaxane and [3]rotaxane.^[a]

Proton	δ ($\Delta\delta$), ppm		
	[8-DB24C8] ²⁺	[8-(DB24C8) ₂] ²⁺	8^{2+}
a	5.51 (+0.42)	5.47 (+0.38)	5.09
b	9.08 (+0.47)	8.95 (+0.34)	8.61
c	8.00 (−0.38)	8.39 (+0.01)	8.38
d	7.76 (−0.36)	8.03 (−0.09)	8.12
e	8.36 (−0.09)	8.52 (+0.07)	8.45
NH	10.87 (−0.01)	11.15 (+0.27)	10.88

^[a] Solution concentration is 1.0×10^{-3} M and temperature 298 K unless otherwise indicated. All anions are BF_4^- .

Again, in contrast to [2]rotaxane [8-DB24C8]²⁺, after two equivalents of acid were added to [8-(DB24C8)₂]²⁺, a symmetrical spectrum was obtained; Figure 6 (bottom). A singlet at 12.9 ppm was observed for the benzimidazolium NH proton which is almost identical to the signal observed for the complexed benzimidazolium NH of [8-H₂C-DB24C8]⁴⁺. The upfield chemical shifting of protons a, f, 1 and 2 further indicates the crown ether wheels are now located on the two benzimidazolium sites of the [3]rotaxane. In other words, the [3]rotaxane shuttling is switched OFF by protonation of the benzimidazole sites.

**Figure 7.** Top, illustration of shuttling of the wheel in [3]rotaxane [8-(DB24C8)₂]²⁺ and bottom, variable temperature NMR spectra of [8-(DB24C8)₂]²⁺ in CD_2Cl_2 .

Conclusions

The combination of benzimidazolium/crown ether and 1,2-bis(pyridinium)ethane/crown ether recognition motifs has been successfully exploited to prepare both [2]rotaxane and [3]rotaxane molecular shuttles. It can be concluded from this new design that: 1) formation of a benzimidazolium group to act as a stopper simultaneously creates a second recognition site, 2) by fine tuning the substituents on the benzimidazolium moiety, the obtained [2]rotaxane can be further developed into an acid/base switchable molecular shuttle, 3) a [3]rotaxane molecular shuttle with unique shuttling dynamics can be produced from the same approach and 4) shuttling of two macrocyclic wheels simultaneously on one single dumbbell can be accomplished. This study may provide new insight for the design of switchable molecular shuttles. Owing to the unique properties of the benzimidazole group, such as fluorescence and coordination to metal ions, these new type molecular shuttles may found further applications in developing functional molecular machines and materials.

Details of X-ray diffraction studies and EXSY experiments including all NMR spectra are available in the Supplementary information accompanying this article.

Experimental Section

General comments: All chemicals were purchased from Aldrich Chemicals and used without further purification. Compounds 4-(4'-formylphenyl)pyridine (**3**)^[20] and 1,2-diamino-3,6-di(4'-t-butylphenyl)-benzene (**6b**)^[19c] were synthesized according to reported methods. Deuterated solvents were obtained from Cambridge Isotope Laboratories and used as received. Solvents were dried using an Innovative Technologies Solvent Purification System. NMR spectra were recorded either on a Bruker Advance 500 or Bruker Advance 300 spectrometer. Chemical shifts are quoted in ppm relative to tetramethylsilane using the residual solvent peak as a reference standard. For the variable temperature experiments, the low temperatures were calibrated using a neat methanol sample. High resolution mass spectrometry (HR-MS) experiments were performed on a Micromass LCT electrospray ionization (ESI) time-of-flight (ToF) mass spectrometer. Solutions with concentrations of 1.0×10^{-3} M were prepared in methanol and injected for analysis at a rate of 5 $\mu\text{L}/\text{min}$ using a syringe pump. Elemental compositions were determined on a PerkinElmer 2400 Series II Elemental Analyzer. All single crystal X-ray data were collected on a Bruker APEX diffractometer with a CCD detector operated at 50 kV and 30 mA with MoK_α radiation. Crystals were frozen in paratone oil inside a cryoloop and reflection data were integrated from frame data obtained from hemisphere scans. The SHELXTL library of programs^[24], Bruker AXS APEX-III^[25] and OLEX2^[26] software were used for data reduction, X-ray solution and refinement while figures were drawn with the CrystalMaker software package.^[27] CCDC 1500508 and 1500509 contain the supplementary crystallographic data for this paper. These data are provided free of charge by the Cambridge Crystallographic Data Centre.

1-Bromoethyl-4-(4'-formylphenyl)pyridinium tetrafluoroborate, [4][BF₄]: 4-(4'-Formylphenyl)pyridine (2.00 g, 0.0109 mol) was dissolved in 1,2-dibromoethane (25 mL) and heated at 65 °C for 48 h. After cooling to room temperature, the reaction mixture was added to CH_2Cl_2 (50 mL) and stirred for 30 min. The solid was filtered, washed with CH_2Cl_2 then

CH₃CN, and air dried. After completely dissolving the solid in hot deionized water (40 mL), a saturated sodium tetrafluoroborate solution (20 mL) was added. The resulting solid was filtered, washed with deionized water, and air dried. Yield: 1.7 g, 41%. MP: 187–189 °C (Decomp.) ¹H NMR (300 MHz, CD₃CN, 298 K) δ = 10.13 (s, 1H), 8.79 (d, 2H, *J* = 6.9 Hz), 8.37 (d, 2H, *J* = 6.9 Hz), 8.11 (m, 4H), 4.95 (t, 2H, *J* = 6.3 Hz), 3.98 (t, 2H, *J* = 7.2 Hz). ¹³C NMR (75 MHz, CDCl₃, 298 K) δ = 193.0, 156.6, 145.8, 139.6, 139.2, 131.1, 130.0, 126.5, 62.2, 31.2. Elemental analysis (%): Calculated for C₁₄H₁₃NOBrBF₄: C, 44.49; H, 3.47; N, 3.71. Found: C, 45.08; H, 3.45; N, 3.65.

2,6-Bis(4-(4'-formylphenyl)-1-pyridyl)ethane tetrafluoroborate, [5][BF₄]₂

1-Bromoethyl-4-(4'-formylphenyl)pyridinium tetrafluoroborate (1.00 g, 0.00265 mol) and 4-(4'-formylphenyl)pyridine (2.43 g, 0.0133 mol) were dissolved in CH₃CN (50 mL) and refluxed for 3 days. After the solvent was removed, the residue was washed with CH₂Cl₂ (20 mL \times 2) and air dried. The solid was anion exchanged to the tetrafluoroborate salt by heating the bromide salt in deionized water and adding NaBF₄. The resulting precipitate was collected by suction filtration, washed with deionized water and air dried. Yield (1.03 g, 68 %). MP: >250 °C (decomp). ¹H NMR (500 MHz, CD₃CN, 298 K) δ = 10.18 (s, 2H), 8.74 (d, 4H, *J* = 7.0 Hz), 8.42 (d, 4H, *J* = 7.0 Hz), 8.19 (d, 4H, *J* = 8.5 Hz), 8.15 (d, 4H, *J* = 8.5 Hz). ¹³C NMR (75 MHz, CD₃CN) δ (ppm) = 192.9, 157.4, 146.0, 139.5, 139.5, 131.2, 130.0, 127.4, 60.0. HR MS (ESI): *m/z* calcd for C₂₇H₂₂N₂O₅F₃S [M-2BF₄ + CF₃SO₃]²⁺: 543.1196; found: 543.1191.

[10][BF₄]₂: [5][BF₄]₂ (503 mg, 0.886 mmol), 1,2-diamino-3,6-di(4'-t-butylphenyl)benzene (**6b**) (110 mg, 0.295 mmol), and ZrCl₄ (7.0 mg, 0.0300 mmol) were stirred in acetonitrile (30 mL) at room temperature for 24 h. After removal of the solvent on a rotary evaporator, the mixture was extracted with hot tetrahydrofuran (30 mL \times 2). Evaporation of the solvent and washing with methanol gave the title compound as a yellow solid. Yield: 166 mg, 61%. Mp 245–248 °C (decomp). ¹H NMR (500 MHz, CD₃CN) δ (ppm) = 10.91 (s, 1H), 10.13 (br s, 1H), 8.72 (d, *J* = 7.0 Hz, 2H), 8.67 (d, *J* = 7.0 Hz, 2H), 8.43 (d, *J* = 8.6 Hz, 2H), 8.41–8.35 (m, 4H), 8.18–8.03 (m, 8H), 7.73 (d, *J* = 7.5 Hz, 2H), 7.64 (d, *J* = 7.5 Hz, 2H), 7.60 (d, *J* = 8.0 Hz, 2H), 7.55 (d, *J* = 7.5 Hz, 1H), 7.42 (d, *J* = 7.5 Hz, 1H), 5.13 (m, 4H), 1.41 (s, 18H). ¹³C NMR (125 MHz, CD₃CN) δ (ppm) = 192.1, 156.9, 156.7, 150.7, 145.2, 144.9, 138.8, 138.7, 134.3, 134.2, 130.5, 129.2, 129.0, 128.8, 128.4, 128.1, 126.6, 126.1, 125.7, 125.3, 123.9, 121.9, 59.4, 59.1, 34.4, 30.6. HRMS (ESI): *m/z* calcd for C₅₂H₅₀N₄O²⁺ [M-2BF₄]²⁺: 373.1987; found: 373.1973.

[10-H][BF₄]₃: Tetrafluoroborate diethyl ether complex (22 μ L, 0.163 mmol) was added to a solution of [10][BF₄]₂ (150 mg, 0.163 mmol) in dichloromethane (5.0 mL). After stirring for 5 min, the solvent was evaporated under vacuum. Yield: 164 mg, quantitative. Mp 203–206 °C (decomp). The product was used directly in the next step. ¹H NMR (500 MHz, CD₃CN) δ = 12.54 (br s, 2H), 10.12 (s, 1H), 8.83 (d, *J* = 6.9 Hz, 2H), 8.80 (d, *J* = 6.9 Hz, 2H), 8.47 (d, *J* = 6.9 Hz, 2H), 8.41 (d, *J* = 6.9 Hz, 2H), 8.30 (d, *J* = 8.5 Hz, 2H), 8.26 (d, *J* = 8.5 Hz, 2H), 8.13 (s, 4H), 7.75 (s, 2H), 7.71 (m, 8H), 5.20 (s, 4H), 1.42 (s, 18H). ¹³C NMR (125 MHz, CD₃CN) δ = 192.2, 156.6, 156.0, 152.3, 150.2, 145.4, 145.3, 138.8, 138.7, 138.5, 132.4, 131.03, 130.4, 120.0, 129.2, 129.2, 128.6, 127.7, 127.4, 126.6, 126.5, 125.1, 117.4, 59.4, 59.3, 34.5, 30.6. HRMS (ESI): *m/z* calcd for C₅₂H₅₀N₄O²⁺ [M-2BF₄-HBF₄]²⁺: 373.1987; found: 373.1973. *m/z* calcd for C₅₄H₅₄N₅O³⁺ [M-3BF₄+CH₃CN]³⁺: 262.8104; found: 262.8055.

[7cDB24C8][BF₄]₂: [5][BF₄]₂ (57.0 mg, 0.100 mmol) and dibenzo[24]-crown-8 (180 mg, 0.400 mmol) were dissolved in acetonitrile (15 mL). After the mixture was stirred at room temperature for 10 min, 1,2-di-isopropoxy-4,5-diaminobenzene (**6a**) (47.0 mg, 0.210 mmol) was added. After the mixture was stirred for 30 min, ZrCl₄ (4.9 mg, 0.0210 mmol) was added. The mixture was allowed to stir open to the air overnight. After the solvent

was removed on a rotary evaporator, the residue was re-dissolved in dichloromethane (50 mL) and washed once with saturated sodium tetrafluoroborate. After removal of the solvent, the residue was washed with diethyl ether. The crude product was purified by flash column chromatography (SiO₂, dichloromethane/methanol, *v/v* = 10:1 to 1:1) to give an orange solid. Yield: 94 mg, 66%. Single crystals were obtained by slow diffusion of di-isopropyl ether into an acetonitrile solution of the compound. MP: >250 °C (decomp). ¹H NMR (500 MHz, CD₃CN, 298 K) δ = 9.09 (d, 4H, *J* = 6.0 Hz), 8.25 (d, 4H, *J* = 7.5 Hz), 8.02 (d, 4H, *J* = 6.5 Hz), 7.78 (d, 4H, *J* = 8.0 Hz), 7.27 (s, 4H), 6.68 (m, 4H), 6.54 (m, 4H), 5.51 (s, 4H), 4.58 (m, 4H), 4.01–4.06 (m, 24H), 1.35 (d, 24H, *J* = 6.0 Hz). ¹³C NMR (75 MHz, CD₃CN, 298 K) δ = 155.0, 148.0, 147.0, 145.7, 134.7, 132.2, 131.8, 129.1, 127.2, 124.0, 123.3, 121.3, 119.1, 112.4, 102.7, 72.3, 70.8, 70.3, 67.8, 57.8, 21.4. HR MS (ESI): *m/z* calcd for C₇₄H₈₆N₆O₁₂ [M-2CF₃SO₃]²⁺: 625.3147; found: 625.3143.

[7][BF₄]₂: The titled compound was isolated as a byproduct from the synthesis of [2]rotaxane [7c(DB24C8)][BF₄]₂. Yield: 22 mg, 23%. MP: 189–192 °C (decomp). ¹H NMR (500 MHz, CD₃CN, 298 K) δ = 8.63 (d, 4H, *J* = 6.5 Hz), 8.37 (d, 4H, *J* = 6.5 Hz), 8.29 (d, 4H, *J* = 8.5 Hz), 8.10 (d, 4H, *J* = 8.5 Hz), 7.18 (s, 4H), 5.11 (s, 4H), 4.55 (m, 4H), 1.33 (d, 24H, *J* = 6.0 Hz). ¹³C NMR (75 MHz, CD₃NO₂, 298 K) δ = 157.2, 148.0, 144.8, 134.6, 132.6, 129.1, 127.4, 125.8, 123.1, 103.0, 72.6, 59.6, 21.1. HRMS (ESI): Due to cleavage of the N-C pyridinium bond, the largest ion observed was the protonated pyridine fragment, *m/z* calcd for C₂₄H₂₆N₃O₂⁺: 388.2020; found: 388.2025.

[8cDB24C8][BF₄]₂: [5][BF₄]₂ (75.0 mg, 0.133 mmol) and dibenzo[24]-crown-8 (240 mg, 0.532 mmol) were dissolved in acetonitrile (20 mL). After the mixture was stirred at room temperature for 10 min, 1,2-diamino-3,6-di(4'-t-butylphenyl)benzene (**6b**) (109 mg, 0.293 mmol) was added. After the mixture was stirred for 30 min, ZrCl₄ (6.2 mg, 0.0260 mmol) was added. The mixture was allowed to stir open to the air overnight. After the solvent was removed on a rotary evaporator, the residue was re-dissolved in dichloromethane (50 mL) and washed with saturated sodium tetrafluoroborate once. After removal of the solvent, the residue was washed with diethyl ether. The crude product was purified by flash column chromatography (SiO₂, dichloromethane/acetone, *v/v* = 3:1) to give a yellow solid. Yield: 73 mg, 32%. Single crystals were obtained by slow evaporation of an acetonitrile solution of the compound. MP: >250 °C (decomp). ¹H NMR (500 MHz, CD₃CN, 298 K) δ = 10.88 (s, 2H), 9.08 (d, 4H, *J* = 7.0 Hz), 8.36 (d, 4H, *J* = 8.5 Hz), 8.13 (d, 4H, *J* = 6.5 Hz), 8.00 (d, 4H, *J* = 7.0 Hz), 7.75–7.77 (m, 8H), 7.66 (d, 4H, *J* = 6.5 Hz), 7.62 (d, 4H, *J* = 6.5 Hz), 7.57 (d, 2H, *J* = 8.0 Hz), 7.44 (d, 2H, *J* = 8.0 Hz), 6.69 (m, 4H), 6.57 (m, 4H), 5.51 (s, 4H), 4.00–4.08 (m, 24H), 1.44 (s, 18H), 1.43 (s, 18H). ¹³C NMR (125 MHz, CD₃CN) δ = 155.4, 150.8, 146.9, 145.6, 135.5, 134.5, 133.6, 128.9, 128.6, 128.0, 124.0, 122.5, 121.2, 117.3, 112.3, 70.7, 70.2, 67.7, 57.4, 34.3, 30.7. HRMS (ESI): *m/z* calcd for C₁₀₂H₁₁₀N₆O₈²⁺ [M-2BF₄]²⁺: 773.9203; found: 773.9353.

[8c(DB24C8)]²⁺: [6-H][BF₄]₃ (101 mg, 0.100 mmol) and dibenzo[24]-crown-8 (270 mg, 0.600 mmol) were dissolved in nitromethane (4.0 mL) and chloroform (8.0 mL). 1,2-Diamino-3,6-di(4'-t-butylphenyl)benzene (**6b**) (41 mg, 0.110 mmol) was added followed by ZrCl₄ (6.2 mg, 0.0260 mmol). The mixture was allowed to stir open to the air overnight. After the solvent was removed on a rotary evaporator, the residue was re-dissolved in dichloromethane (50 mL) and washed once with a saturated sodium tetrafluoroborate solution. After removal of the solvent, the residue was washed with diethyl ether and air dried. Methanol (10 mL) was added and the insoluble solid was filtered off. Upon adding trimethylamine (0.1 mL) to the filtrate, a yellow solid was precipitated. The solid was filtered by vacuum suction and washed with cold methanol and air dried. Slow evaporation of a dichloromethane/ethyl acetate solution afforded the pure product as a yellow solid. Yield: 91 mg, 42%. MP: >250 °C (decomp). ¹H

NMR (500 MHz, CD₃CN) δ = 11.15 (s, 2H), 8.96 (d, J = 6.8 Hz, 4H), 8.52 (d, J = 8.3 Hz, 4H), 8.39 (d, J = 5.7 Hz, 4H), 8.17 (d, J = 8.3 Hz, 4H), 8.03 (d, J = 8.1 Hz, 4H), 7.71 (d, J = 8.1 Hz, 4H), 7.59 (d, J = 7.7 Hz, 2H), 7.55 (m, 8H), 7.43 (d, J = 7.7 Hz, 2H), 6.85 (m, 16H), 5.47 (s, 4H), 4.06 (m, 16H), 3.69 (s, 16H), 3.33 (m, 8H), 3.20 (m, 8H), 1.40 (s, 18H), 1.39 (s, 18H). ¹³C NMR (125 MHz, CD₃CN, 298 K) δ = 155.3, 151.3, 148.7, 147.4, 144.3, 134.3, 133.5, 129.2, 128.9, 125.9, 125.2, 125.0, 121.3, 121.2, 114.2, 112.0, 70.1, 69.6, 68.0, 57.4, 34.2, 30.6. HRMS (ESI): m/z calcd for C₁₂₆H₁₄₃N₆O₁₆³⁺ [M-2BF₄+H]³⁺: 665.6859; found: 665.6862.

[8][BF₄]₂: A mixture of [5][BF₄]₂ (57 mg, 0.100 mmol), 1,2-diamino-3,6-di(4'-t-butylphenyl)benzene (**6b**) (82 mg, 0.220 mmol) and ZrCl₄ (4.7 mg, 0.0200 mmol) in 20 mL of acetonitrile/CHCl₃ (v/v=4:1) was stirred at room temperature overnight. The yellow precipitate was filtered and re-dissolved in nitromethane (30 mL). After washing once with a saturated sodium tetrafluoroborate solution, the solvent was removed. The crude product was further purified by washing with methanol. Yield: 103 mg, 81%. MP: 223–226 °C (decomp). ¹H NMR (500 MHz, CD₃CN, 298 K) δ = 10.88 (s, 2H), 8.61 (d, 4H, J = 7.0 Hz), 8.45 (d, 4H, J = 8.5 Hz), 8.38 (d, 4H, J = 7.0 Hz), 8.10–8.13 (m, 8H), 7.74 (d, 4H, J = 8.5 Hz), 7.64 (d, 4H, J = 8.5 Hz), 7.60 (d, 4H, J = 7.0 Hz), 7.56 (d, 2H, J = 7.5 Hz), 7.43 (d, 2H, J = 7.5 Hz), 5.09 (s, 4H), 1.42 (s, 18H), 1.41 (s, 18H). ¹³C NMR (125 MHz, DMSO-*d*₆, 298 K) δ = 155.2, 151.3, 150.6, 150.2, 145.8, 142.5, 135.7, 135.5, 134.4, 134.2, 134.2, 130.4, 129.1, 128.9, 128.6, 126.2, 125.6, 125.6, 125.1, 124.3, 121.9, 59.4, 34.8, 31.6. HRMS (ESI): m/z calcd for C₇₈H₇₈N₆ [M-2BF₄]²⁺: 549.3138; found: 549.3137.

Acknowledgements

SJL is grateful for the awarding of NSERC of Canada Discovery grants in support of this research. SJL also thanks the Canadian Foundation for Innovation, the Ontario Innovation Trust and the University of Windsor for support of the X-ray diffraction at the University of Windsor. Additional support was provided to SJL through the NSERC Canada Research Chair (CRC) program.

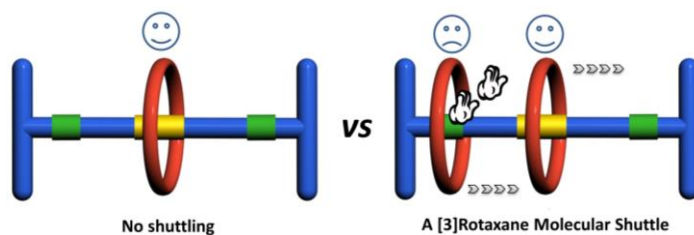
Keywords: rotaxane • molecular shuttle • molecular switch • benzimidazole • supramolecular chemistry

- [1] a) J-P. Sauvage, C. Dietrich-Buchecker, (eds) *Molecular Catenanes, Rotaxanes and Knots: A Journey Through the World of Molecular Topology* (Wiley-VCH, 1999); b) E. K. Kay, D. A. Leigh, F. Zerbetto, *Angew. Chem. Int. Ed.* **2007**, *46*, 72; c) V. Balzani, *Pure Appl. Chem.* **2008**, *80*, 1631; d) M. J. Langton, P. D. Beer, *Acc. Chem. Res.* **2014**, *47*, 1935; e) J. F. Stoddart, *Angew. Chem. Int. Ed.* **2014**, *53*, 11102; f) K. Zhu, S. J. Loeb, *Top. Curr. Chem.*, **2014**, *354*, 213; g) S. Erbas-Cakmak, D. A. Leigh, C. T. McTernan, A. L. Nussbaumer, *Chem. Rev.*, **2015**, *115*, 10081.
- [2] a) P. Thordarson, E. J. A. Bijsterveld, A. E. Rowan, R. J. M. Nolte, *Nature*, **2003**, *424*, 915-918; b) B. Lewandowski, G. De Bo, J. W. Ward, M. Papmeyer, S. Kuschel, M. J. Aldegunde, P. M. E. Gramlich, D. Heckmann, S. M. Goldup, D. M. D'Souza, A. E. Fernandes and D. A. Leigh, *Science*, **2013**, *339*, 189-193; c) G. De Bo, S. Kuschel, D. A. Leigh, B. Lewandowski, M. Papmeyer, J. W. Ward, *J. Am. Chem. Soc.*, **2014**, *136*, 5811–5814.
- [3] a) Y. Tachibana, N. Kihara, T. Takata, *J. Am. Chem. Soc.* **2004**, *126*, 3438–3439; b) G. Attori, T. Hori, Y. Miyake, Y. Nishibayashi, *J. Am. Chem. Soc.* **2007**, *129*, 12930–12931; c) Y. Suzaki, K. Shimada, E. Chihara, T. Saito, Y. Tsuchido, K. Osakada, *Org. Lett.* **2011**, *13*, 3774–3777; d) C. B. Caputo, K. Zhu, V. N. Vukotic, S. J. Loeb, D. W. Stephan, *Angew. Chem., Int. Ed.* **2013**, *52*, 960–963; e) V. Blanco, D. A. Leigh, V. Marcos, J. A. Morales-Serna, A. L. Nussbaumer, *J. Am. Chem. Soc.* **2014**, *136*, 4905–4908.
- [4] a) N. D. Suhan, L. Allen, M. T. Gharib, E. Viljoen, S. J. Vella, S. J. Loeb, *Chem. Commun.*, **2011**, *47*, 5991–5993; b) M. J. Langton, S. W. Robinson, I. Marques, V. Félix, P. D. Beer, *Nat. Chem.*, **2014**, *6*, 1039–1043; c) X. Hou, C. Ke, C. J. Bruns, P. R. McGonigal, R. B. Pettman, J. F. Stoddart, *Nat. Commun.* **2015**, *6*, 6884; d) Z. Cao, Q. Miao, Q. Zhang, H. Li, D. Qu, H. Tian, *Chem. Commun.*, **2015**, *51*, 4973–4976; e) X. Ma, J. Zhang, J. Cao, X. Yao, T. Cao, Y. Gong, C. Zhao, H. Tian, *Chem. Sci.*, **2016**, *7*, 4582–4588.
- [5] a) N. Yui, R. Katoono, A. Yamashita, *Adv. Polym. Sci.* **2009**, *222*, 115–173; b) K. K. Coti, M. E. Belowich, M. L., M. W. Ambrogio, Y. A. Lau, H. A. Khatib, J. I. Zink, N. M. Khashab, J. F. Stoddart, *Nanoscale* **2009**, *1*, 16–39; c) M. Liong, S. Angelos, E. Choi, K. Patel, J. F. Stoddart, J. I. Zink, *J. Mater. Chem.* **2009**, *19*, 6251–6257; d) R. Barat, T. Legigan, I. Tranoy-Opalinski, B. Renoux, E. Péraudeau, J. Clarhaut, P. Poinot, A. E. Fernandes, V. Aucagne, D. A. Leigh, S. Papot, *Chem Sci*, **2015**, *6*, 2608–2613.
- [6] a) I. Aprahamian, T. Yasuda, T. Ikeda, S. Saha, W. R. Dichtel, K. Isoda, T. Kato, J. F. Stoddart, *Angew. Chem. Int. Ed.* **2007**, *119*, 4759–4763; b) T. Yasuda, K. Tanabe, T. Tsuji, K. K. Coti, I. Aprahamian, J. F. Stoddart, T. Kato, *Chem. Commun.* **2010**, *46*, 1224–1226; c) N. D. Suhan, S. J. Loeb, S. H. Eichhorn, *J. Am. Chem. Soc.*, **2013**, *135*, 400–408; d) H. He, E. M. Seveck, D. R. M. Williams, *Chem. Commun.*, **2015**, *51*, 16541–16544.
- [7] a) T. Oku, Y. Furusho, T. Takata, *Angew. Chem. Int. Ed. Engl.* **2004**, *43*, 966–996; b) K. Mayumi, K. Ito, *Polymer*, **2010**, *51*, 959–967; c) S. Li, J. Chen, B. Zheng, S. Dong, Z. Ma, H. W. Gibson, F. Huang, *J. Polym. Sci. Pol. Chem.* **2010**, *48*, 4067–4073; G. Du, E. Moulin, N. Jouault, E. Buhler, N. Giuseppone, *Angew. Chem. Int. Ed.* **2012**, *51*, 12504.
- [8] a) K. Galatsis, K. Wang, Y. Botros, Y. Yang, Y. H. Xie, J. F. Stoddart, R. B. Kaner, C. Ozkan, J. L. Liu, M. Ozkan, C. W. Zhou, K. W. Kim, *IEEE Circuits & Devices* **2006**, *22*, 12–21; b) J. E. Green, J. W. Choi, A. Boukai, Y. Bunimovich, E. Johnston-Halprin, E. Delonno, Y. Luo, B. A. Sheriff, K. Xu, Y. S. Shin, H. -R. Tseng, J. F. Stoddart, J. R. Heath, *Nature* **2007**, *445*, 414–417.
- [9] a) G. J. E. Davidson, S. J. Loeb, *Angew. Chem. Int. Ed. Engl.*, **2003**, *42*, 74–77; b) S. J. Loeb, *Chem. Soc. Rev.* **2007**, *36*, 226; c) Q. Li, C.-H. Sue, S. Basu, A. K. Shveyd, W. Zhang, G. Barin, L. Fang, A. Sarjeant, J. F. Stoddart, O. M. Yaghi, *Angew. Chem. Int. Ed.* **2010**, *49*, 6751–6755; d) V. N. Vukotic, S. J. Loeb, *Chem. Soc. Rev.*, **2012**, *41*, 5896–5906; e) V. N. Vukotic, K. J. Harris, K. Zhu, R. W. Schurko, S. J. Loeb, *Nat. Chem.*, **2012**, *4*, 456–460; f) K. Zhu, V. N. Vukotic, C. A. O'Keefe, R. W. Schurko, and S. J. Loeb, *J. Am. Chem. Soc.*, **2014**, *136*, 7403–7409; g) P. R. McGonigal, P. Deria, I. Hod, P. Z. Moghadam, A.-J. Avestro, N. E. Horwitz, I. C. Gibbs-Hall, A. K. Blackburn, D. Chen, Y. Y. Botros, W. R. Wasielewski, R. Q. Snurr, J. T. Hupp, O. K. Farha, J. F. Stoddart, *Proc. Natl. Acad. Sci. USA* **2015**, *112*, 11161–11168; h) V. N. Vukotic, C. A. O'Keefe, K. Zhu, K. J. Harris, C. To, R. W. Schurko, and S. J. Loeb, *J. Am. Chem. Soc.*, **2015**, *137*, 9643–9651; i) K. Zhu, C. O'Keefe, V. N. Vukotic, R. W. Schurko, S. J. Loeb, *Nat. Chem.*, **2015**, *7*, 514–519; j) N. Farahani, K. Zhu, C. A. O'Keefe, R. W. Schurko, S. J. Loeb, *ChemPlusChem*, **2016**, *81*, 836–841.
- [10] a) F. Arico, J. D. Badjic, S. J. Cantrill, A. H. Flood, K. C.-F. Leung, Y. Liu, J. F. Stoddart, *Top. Curr. Chem.*, **2005**, *249*, 203–259; b) J. E. Beves, B. A. Blight, C. J. Campbell, D. A. Leigh, R. T. McBurney, *Angew. Chem. Int. Ed.*, **2011**, *50*, 9260–9327.
- [11] a) H. M. Colquhoun, E. P. Goodings, J. M. Maud, J. F. Stoddart, D. J. Williams, J. B. Wolstenholme, *J. Chem. Soc., Chem. Commun.* **1983**, *20*, 1140–1142; b) P. R. Ashton, D. Philp, M. V. Reddington, A. M. Z. Slawin, N. Spencer, J. F. Stoddart, D. J. Williams, *J. Chem. Soc., Chem. Commun.* **1991**, *23*, 1680–1683; c) S. J. Loeb, J. A. Wisner, *Angew. Chem. Int. Ed.* **1998**, *37*, 2838–2840; d) T. Han, C.-F. Chen, *Org. Lett.* **2007**, *9*, 4207; e) C. He, Z. Shi, Q. Zhou, S. Li, N. Li, F. Huang, *J. Org. Chem.*, **2008**, *73*, 5872; f) A. M.-P. Pederson, E. M. Ward, D. V.

- Schoonover, C. Slebodnick, H. W. Gibson, *J. Org. Chem.*, **2008**, *73*, 9094; g) X. Yan, P. Wei, M. Zhang, X. Chi, J. Liu, F. Huang, *Org. Lett.*, **2011**, *13*, 6370.
- [12] a) S. J. Loeb, J. A. Wisner, *Chem. Commun.*, **1998**, 2757–2758; b) G. J. E. Davidson, S. J. Loeb, N. A. Parekh, J. A. Wisner, *J. Chem. Soc., Dalton Trans.*, **2001**, 3135–3136; c) N. Georges, S. J. Loeb, J. Tiburcio, J. A. Wisner, *Org. Biomol. Chem.*, **2004**, *2*, 2751–2756; d) D. J. Mercer, J. Yacoub, K. Zhu, S. K. Loeb, S. J. Loeb, *Org. Biomol. Chem.*, **2012**, *10*, 6094–6104; e) D. J. Mercer, S. J. Loeb, *Dalton Trans.*, **2011**, *40*, 6386–6387.
- [13] S. J. Loeb, J. A. Wisner, *Chem. Commun.*, **2000**, 845–846.
- [14] A. L. Hubbard, G. J. E. Davidson, R. H. Patel, J. A. Wisner, S. J. Loeb, *Chem. Commun.*, **2004**, 138–139.
- [15] S. J. Loeb, J. A. Wisner, *Chem. Commun.*, **2000**, 1939–1940.
- [16] S. J. Loeb, D. A. Tramontozzi, *Org. Biomol. Chem.*, **2005**, *3*, 1393.
- [17] a) S. J. Loeb, *Chem. Commun.* **2005**, 1511–1518; b) S. J. Loeb, *Chem. Soc. Rev.*, **2007**, *36*, 226–235; c) V. N. Vukotic, S. J. Loeb, *Chem. Eur. J.*, **2010**, *16*, 13630–13637; d) D. J. Mercer, V. N. Vukotic, S. J. Loeb, *Chem. Commun.*, **2011**, *47*, 896–898; e) L. K. Knight, V. N. Vukotic, E. Viljoen, C. B. Caputo, S. J. Loeb, *Chem. Commun.*, **2009**, 5585–5587.
- [18] a) D. Castillo, P. Astudillo, J. Mares, F. J. González, A. Vela, J. Tiburcio, *Org. Biomol. Chem.*, **2007**, *5*, 2252; b) L. Li, G. J. Clarkson, *Org. Lett.*, **2007**, *9*, 497; c) M. Lee, Z. Niu, D. V. Schoonover, C. Slebodnick, H. W. Gibson, *Tetrahedron* **2010**, *66*, 7077–7082; d) S. Dong, J. Yuan, F. Huang, *Chem. Sci.*, **2014**, *5*, 247–252.
- [19] a) N. Noujeim, K. Zhu, V. N. Vukotic, S. J. Loeb, *Org. Lett.*, **2012**, *14*, 2484–2487; b) K. Zhu, V. N. Vukotic, S. J. Loeb, *Angew. Chem. Int. Ed.*, **2012**, *51*, 2168–2172; c) K. Zhu, V. N. Vukotic, N. Noujeim, S. J. Loeb, *Chem. Sci.*, **2012**, *3*, 3265–3271; d) N. Farahani, K. Zhu, N. Noujeim, S. J. Loeb, *Org. Biomol. Chem.* **2014**, 4824–4827; e) N. Farahani, K. Zhu, S. J. Loeb, *ChemPhysChem* **2016**, *17*, 1875–1880.
- [20] R. Mueller, M. Huerzeler, C. Boss, *Molecules*, **2003**, *8*, 556.
- [21] S. J. Loeb, J. Tiburcio, S. J. Vella, J. A. Wisner, *Org. Biomol. Chem.*, **2006**, *4*, 667–680.
- [22] C. L. Perrin, T. J. Dwyer, *Chem. Rev.*, **1990**, *90*, 935.
- [23] Similar behavior has been observed for neutral molecular shuttles which have residual hydrogen bonding between benzimidazole NH and crown ether O atoms; see reference [19c].
- [24] G. M. Sheldrick, *Acta Cryst.* **2008**, *A64*, 112–115.
- [25] APEX3: v2016.1-0, Copyright 2003, 2004; Bruker Nonius, Copyright 2005–2016 Bruker AXS.
- [26] O. V. Dolomanov, L. J. Bourhis, R. J. Gildea, J. A. K. Howard, H. Puschmann, *OLEX2: J. Appl. Cryst.*, **2009**, *42*, 339–340.
- [27] Images generated using CrystalMaker®; *CrystalMaker Software Ltd*, Oxford, England (www.crystallmaker.com).

FULL PAPER

[3]Rotaxane molecular shuttle: translocating two macrocyclic wheels simultaneously on one single dumbbell-shaped axle.



Kelong Zhu^{*[a]}, V.
Nicholas Vukotic^[b] and
Stephen J. Loeb^{*[b]}

Page No. – Page No.

Acid-Base Switchable
[2]- and [3]Rotaxane
Molecular Shuttles with
Benzimidazolium and
Bis(pyridinium)
Recognition Sites